

Chiral pair density wave as a precursor of the pseudogap in kagomé superconductors

Narayan Mohanta

Department of Physics, Indian Institute of Technology Roorkee, Roorkee 247667, India

Motivated by scanning tunneling microscopy experiments on AV_3Sb_5 ($A = \text{Cs, Rb, K}$) that revealed periodic real-space modulation of electronic states at low energies, I show using model calculations that a triple- \mathbf{Q} chiral pair density wave (CPDW) is generated in the superconducting state by a charge order of $2a \times 2a$ superlattice periodicity, intertwined with a time-reversal symmetry breaking orbital loop current. In the presence of such a charge order and orbital loop current, the superconducting critical field is enhanced beyond the Chandrasekhar-Clogston limit. The CPDW correlation survives even when the long-range superconducting phase coherence is diminished by a magnetic field or temperature, stabilizing an exotic granular superconducting state above and in the vicinity of the superconducting transition. The presented results suggest that the CPDW can be regarded as the origin of the pseudogap observed near the superconducting transition.

Understanding electronic properties arising from coexisting superconductivity and various density-wave orders has remained as a central problem in condensed matter physics. It has captivated the physics community for decades in the context of high-temperature cuprate superconductors; the recently-synthesized kagomé metals AV_3Sb_5 ($A = \text{Cs, Rb, K}$) have revived the interest [1]. The V atoms in these compounds form a kagomé lattice, and the Fermi level is predominantly populated by V $3d$ orbitals. The electronic band structure exhibits Dirac points and nearly-flat less-dispersive bands [2, 3]. Strong correlation of the nearly-flat bands, topological effects from the Dirac fermions, van Hove singularities, and frustration effects in the kagomé geometry are favorable conditions for instabilities towards long-range many-body order to set in. Superconductivity with a gap-to- T_c ratio $2\Delta_0/k_B T_c \approx 5$ was found below $T_c \approx 2.5$ K [2]. A chiral charge order was found to appear below $T_{co} \approx 94$ K with broken time-reversal symmetry (TRS) but without the trace of any long-range magnetic order, indicating the presence of an intertwined orbital loop current [4–6]. The absence of acoustic phonon anomaly at the charge-order wave vector rules out the Pierls instability related to the Fermi surface nesting and phonon softening as a possible mechanism, and implies that extended Coulomb interactions at a van Hove filling may be responsible for it [7–9]. A pressure-driven transition from fully-gapped to partially-gapped superconductivity and the coexistence of the superconductivity with the charge order over a large parameter regime suggest unconventional pairing in these compounds [10]. Alternative scenarios include non-chiral, anisotropic s -wave superconductivity, supported by recent experimental findings at different pressures [11].

A suppressed electronic density of states at the Fermi level, known as the ‘pseudogap’, posed an enigmatic problem in the high-temperature cuprate superconductors. A similar pseudogap with a V-shaped density of states was observed in scanning tunneling microscopy experiments on AV_3Sb_5 and subsequent theoretical analysis, with periodic modulations of both charge density and

Cooper pair density of $2a \times 2a$ superlattice periodicity (a being the lattice constant) [12–15]. The findings are usually indicative of a nodal pairing symmetry or ungapped sections of the Fermi surface. The concomitant periodic modulations of both superfluid and normal fluid raised a series of questions including the origin of the pseudogap found in the tunneling spectra.

Here, I focus on the observed variation of the density of states in the pseudogap near the superconducting transition and show that a chiral density wave of s -wave Cooper pairs can account for it. The chiral pair density wave (CPDW) is generated in the superconducting state by the TRS breaking charge order and it persists above the superconducting transition without long-range superconducting phase coherence. This CPDW state can be described by a pairing gap $\Delta(\mathbf{r}) = \sum_a \Delta_a e^{i(\mathbf{Q}_a \cdot \mathbf{r} + \varphi_a)}$ at a lattice site position \mathbf{r} , Δ_a and φ_a being the magnitude and the relative phase of the pairing amplitude along three characteristic momentum \mathbf{Q}_a ($a = 1, 2, 3$), set by the charge order periodicity. The presented theoretical arguments are based on calculated density of states $\rho(E)$ and Fourier transformed local density of states $\rho(\mathbf{Q}_p, E)$ at a CPDW wave vector \mathbf{Q}_p . In the vicinity and above the critical field B_c or critical temperature T_c for the superconducting transition, determined by a vanishing superfluid density n_s , $\rho(\mathbf{Q}_p, E)$ reveals a particle-hole symmetric density of states around zero energy, thereby ruling out the charge-ordered electronic states as a possible origin of the pseudogap. Remarkably, the critical value of the magnetic field, perpendicular to the kagomé plane, is found to be enhanced beyond the usual Chandrasekhar-Clogston limit in the presence of the orbital loop current, implying that a highly-provoking quantum state prevails above the superconducting transition.

Two types of charge order were reported—star of David and tri-hexagonal or inverse star of David patterns, both of $2a \times 2a$ periodicity [16–18]. A chiral flux phase, compatible with the symmetry of the kagomé lattice and broken TRS, was shown to be energetically favorable [19]. The tri-hexagonal charge order which has been observed

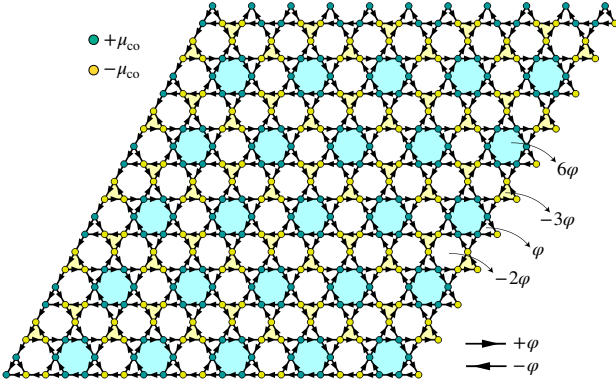


FIG. 1. Charge order configuration with intertwined orbital loop current on the kagomé lattice, analogous to the tri-hexagonal pattern observed in experiments. The yellow and cyan colors represent the modulation in the chemical potential μ_{co} , while the arrows represent the loop current propagation direction and the associated flux φ .

prominently in most compounds, as shown in Fig. 1, is considered in the theoretical model and results presented below. Such an unusual charge ordered state is also supported by a number of interesting phenomena such as anomalous Hall effect and Nernst effect [20–22].

Model and observables.—To model the superconducting state and the experimentally-observed pseudogap, the minimal tight-binding Hamiltonian at the mean spin-singlet pairing field on the kagomé lattice is expressed as

$$\mathcal{H} = -t \sum_{\langle ij \rangle, \sigma} (c_{i\sigma}^\dagger c_{j\sigma} + \text{H.c.}) - \sum_{i, \sigma} (\mu_0 + \xi_i \mu_{co}) c_{i\sigma}^\dagger c_{i\sigma} \quad (1)$$

$$- \sum_i (\Delta_i c_{i\uparrow}^\dagger c_{i\downarrow}^\dagger + \text{H.c.}) - it_{lc} \sum_{\langle ij \rangle, \sigma} (c_{i\sigma}^\dagger c_{j\sigma} - \text{H.c.}),$$

where t is the nearest-neighbor hopping energy, μ_0 is the global chemical potential, μ_{co} is the charge order amplitude, ξ_i is a local variable (± 1) that generates the tri-hexagonal charge order pattern, shown in Fig. 1, Δ_i is the local spin-singlet pairing gap, and the complex nearest-neighbor hopping it_{lc} incorporates the TRS breaking orbital loop current. The Hamiltonian is diagonalized by using the standard unitary transformation of the fermionic fields $c_{i\sigma} = \sum_n u_{ni}^\sigma \gamma_n + v_{ni}^{\sigma*} \gamma_n^\dagger$, where γ_n is an annihilation operator acting on the n^{th} eigenstate, and u_{ni}^σ (v_{ni}^σ) is the corresponding quasiparticle (quasi-hole) amplitude at site i and spin σ . The eigenstates are obtained by solving the Bogoliubov-de Gennes equations $\sum_j \mathcal{H}_{ij} \psi_{nj} = E_n \psi_{ni}$, subject to the self-consistent gap equation [23]

$$\Delta(\mathbf{r}_i) = \frac{\mathcal{U}}{2} \sum_n [u_{ni}^\uparrow v_{ni}^{\downarrow*} - u_{ni}^\downarrow v_{ni}^{\uparrow*}] \tanh\left(\frac{E_n}{2k_B T}\right), \quad (2)$$

where $\psi_{ni} = [u_{ni}^\uparrow, u_{ni}^\downarrow, v_{ni}^\uparrow, v_{ni}^\downarrow]^T$, \mathcal{U} is the pair-wise attractive potential and T is the temperature. Throughout the presented results, μ_0 is kept at zero which places the

Fermi level close to one of the van Hove singularities, $t=1$ and $\mathcal{U}=2$. The relevant energy scale is the maximum pairing gap magnitude, which was found experimentally to be $\Delta \approx 0.52$ meV [13], is taken here to be the unit for all energies in what follows.

To keep track of the superconducting transition, the global superconducting phase rigidity, determined by the superfluid density, is calculated from the effective Drude weight, given by [1, 23]

$$n_s = \frac{D_s}{\pi e^2} = -\langle \kappa \rangle + \Lambda(\mathbf{Q} \rightarrow 0, i\omega \rightarrow 0), \quad (3)$$

where the first term on the right hand side is the diamagnetic response, with the local kinetic energy expressed in terms of the Bogoliubov quasiparticle weights as

$$\kappa_i = -t \sum_{\langle j \rangle, n, \sigma} [u_{ni}^\sigma u_{nj}^{\sigma*} + \text{c.c.}] f(E_n) + [v_{ni}^\sigma v_{nj}^{\sigma*} + \text{c.c.}] (1 - f(E_n)). \quad (4)$$

The second term represents the paramagnetic response, obtained by the transverse current-current correlation function

$$\Lambda(\mathbf{Q} \rightarrow 0, i\omega \rightarrow 0) = \frac{1}{N} \sum_{i, j, n_1, n_2}^{\sigma, \sigma'} \mathcal{A}_{n_1 n_2}^{i\sigma\sigma'} [\mathcal{A}_{n_1 n_2}^{j\sigma\sigma'*} + \mathcal{B}_{n_1 n_2}^{j\sigma\sigma'}] \times \frac{f(E_{n_1}) - f(E_{n_2})}{E_{n_1} - E_{n_2}}, \quad (5)$$

where N is the total number of lattice sites and

$$\mathcal{A}_{n_1 n_2}^{i\sigma\sigma'} = 2[u_{n_1 i}^{\sigma'*} u_{n_2 i}^\sigma - u_{n_1 i}^{\sigma*} u_{n_2 j}^{\sigma'}],$$

$$\mathcal{B}_{n_1 n_2}^{i\sigma\sigma'} = 2[v_{n_1 i}^{\sigma'*} v_{n_2 i}^\sigma - v_{n_1 i}^{\sigma*} v_{n_2 j}^{\sigma'}]. \quad (6)$$

The local density of states, an observable that can be compared with the scanning tunneling microscopy data, is calculated via

$$\rho(\mathbf{r}_i, E) = \sum_n [|u_{ni}^\sigma|^2 \delta(E - E_n) + |v_{ni}^\sigma|^2 \delta(E + E_n)]. \quad (7)$$

The total density of states $\rho(E)$ is obtained by summing over all lattice sites, and the Fourier transformed local density of states at a momentum \mathbf{Q} is obtained using

$$\rho(\mathbf{Q}, E) = \frac{1}{N} \sum_i \cos(\mathbf{Q} \cdot \mathbf{r}_i) \rho(\mathbf{r}_i, E). \quad (8)$$

The local and non-local modulations of the density of states are useful to analyze the presence of the particle-hole symmetry and hence, to differentiate the contributions from the normal fluid and the superfluid, as will be evident from the numerical results presented below.

The CPDW state.—The density wave of s -wave bosons is envisaged from the pairing gap $\Delta(\mathbf{r}_i) = \Delta_m e^{i\theta_i}$, both real and imaginary parts of which reveal $2a \times 2a$ periodic modulation (real part is shown on the color scale in Fig. 2(a)). The phase angle θ_i also shows a periodic structure (arrows in Fig. 2(a)). This intriguing CPDW state is confirmed further by the Fourier transform of the

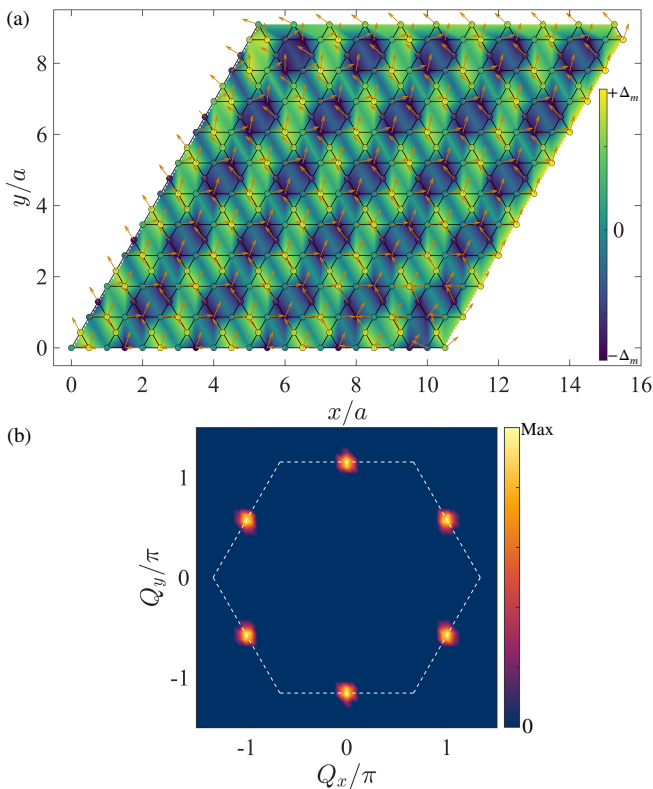


FIG. 2. (a) Profile of the pairing gap $\Delta(\mathbf{r}_i) = \Delta_m e^{i\theta_i}$ solution on the considered $10a \times 10a$ lattice with periodic boundary conditions—the color scale shows the real part; the arrows show the phase θ_i . (b) Fourier transform of the pair-pair correlation function $C(\mathbf{Q})$ obtained on a $20a \times 20a$ lattice with periodic boundary conditions, showing the three characteristic momenta (six-peak structure), indicative of the CPDW state. The hexagon plotted with dashed lines depicts the Brillouin zone. Parameters used are $\mu_{co} = 0.5$ and $t_{lc} = 1$.

pair-pair correlation function

$$C(\mathbf{Q}) = \frac{1}{N} \sum_{i,j} \langle \Delta(\mathbf{r}_i) \Delta(\mathbf{r}_j) \rangle e^{-i\mathbf{Q} \cdot \mathbf{r}_{ij}}, \quad (9)$$

which shows three characteristic momenta (see Fig. 2(b)), given by $(\pm\pi, \pi/\sqrt{3})$ and $(0, 2\pi/\sqrt{3})$. It is confirmed that the CPDW state is generated in the superconducting state due to the interplay between s -wave onsite pairing, charge order and the TRS breaking orbital loop current. Three types of such triple- \mathbf{Q} correlation, at different momenta, have been observed in the experiments [12, 13], implying that the density waves are cascaded between normal fluid and superfluid *i.e.* the CPDW can also induce subsequent charge orders.

Pseudogap.—The coexistence of charge order and superconductivity in AV_3Sb_5 over a large parameter regime raised the natural question whether there is a cooperation between the two commonly-known competing orders [25]. The present analysis shows that the superconducting gap is suppressed in the presence of the charge order and the orbital loop current at zero temperature

and zero magnetic field. However, the average pairing gap $|\Delta|$ vanishes at a magnetic field and a temperature, larger than the critical values B_c and T_c , determined by a vanishing superfluid density n_s (Fig. 3(a)-(b)). The magnetic field of amplitude B_z was incorporated by the Hamiltonian $\mathcal{H}_z = -\mu_B B_z \sum_{i,\sigma,\sigma'} \sigma_{\sigma\sigma'}^z c_{i\sigma}^\dagger c_{i\sigma'}$ which describes the Zeeman exchange coupling. Remarkably, the critical field at which $|\Delta|$ drops to zero is enhanced by more than 20% above B_c in the presence of the charge order and the loop current. It is known that a conventional spin-singlet superconductor, with a gap around the Fermi level, has a vanishing paramagnetic susceptibility at $T = 0$, and hence it cannot lower its Free energy indefinitely by spin-polarizing the quasiparticle states in the presence of a Zeeman magnetic field. Consequently, when the Zeeman energy gain is comparable to the superconducting condensation energy, given by $\mu_B B_{c0} = \Delta_0/\sqrt{2} \approx 0.7\Delta_0$, known as the Chandrasekhar-Clogston limit [26, 27], there is a transition to the normal state. An exception to this stringent condition occurs in the case of Fulde-Ferrell-Larkin-Ovchinnikov type finite-momentum condensates [28, 29] and in thin superconducting films with a large spin-orbit coupling [30]. The enhancement in the critical field for vanishing $|\Delta|$ in the kagomé lattice with a charge order and orbital loop cur-

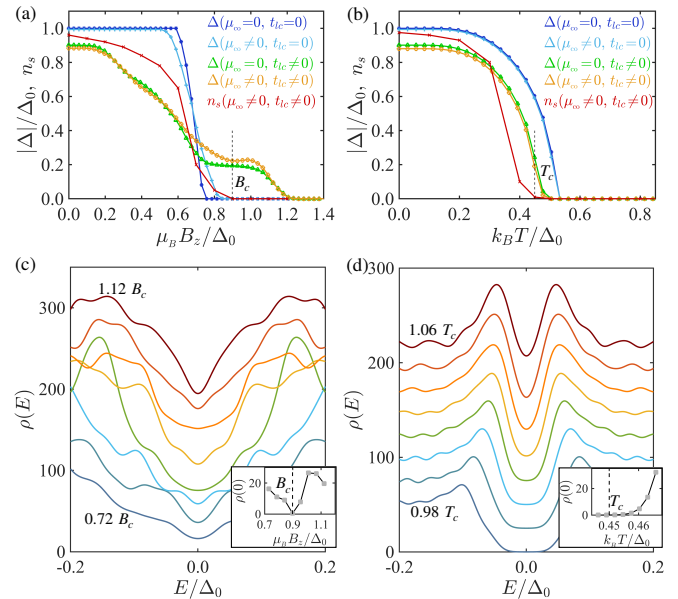


FIG. 3. (a), (b) Variation of the average gap magnitude $|\Delta|$ (without and with the charge order and the loop current) and superfluid density n_s with magnetic field B_z and temperature T . (c), (d) Density of states $\rho(E)$ for different B_z and T near the critical values B_c and T_c , determined by vanishing n_s . Insets in (c), (d) show the density of states at zero energy $\rho(0)$ as a function of B_z and T , respectively. The results were obtained on a $20a \times 20a$ lattice with periodic boundary conditions. All other parameters are the same as in Fig. 2. A constant offset has been added to the vertical axis for each curve in (c) and (d) for clarity.

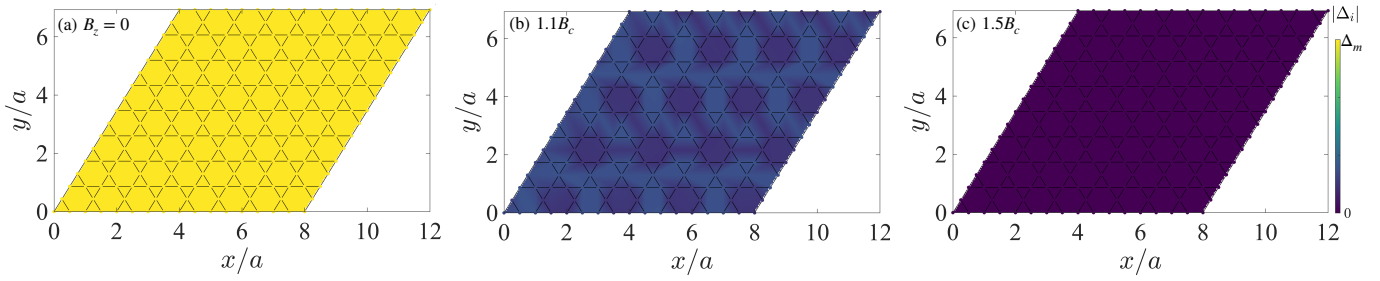


FIG. 4. Profile of the absolute value of the pairing gap $|\Delta(\mathbf{r}_i)|$, self-consistently obtained on a $8a \times 8a$ lattice with periodic boundary conditions, at different magnetic fields across the superconducting transition: (a) $B_z = 0$, (b) $B_z = 1.1B_c$, and (c) $B_z = 1.5B_c$. In the vicinity of the superconducting transition (the case of plot (b)), the pairing gap is locally suppressed in the charge-ordered clusters, creating a granular phase having superconducting patches separated by non-superconducting regions. All other parameters are the same as in Fig. 2.

rent indicates the formation of an unconventional state above and in the vicinity of the superconducting transition. However, it can be attributed to the non-zero density of states $\rho(E)$ within the superconducting gap

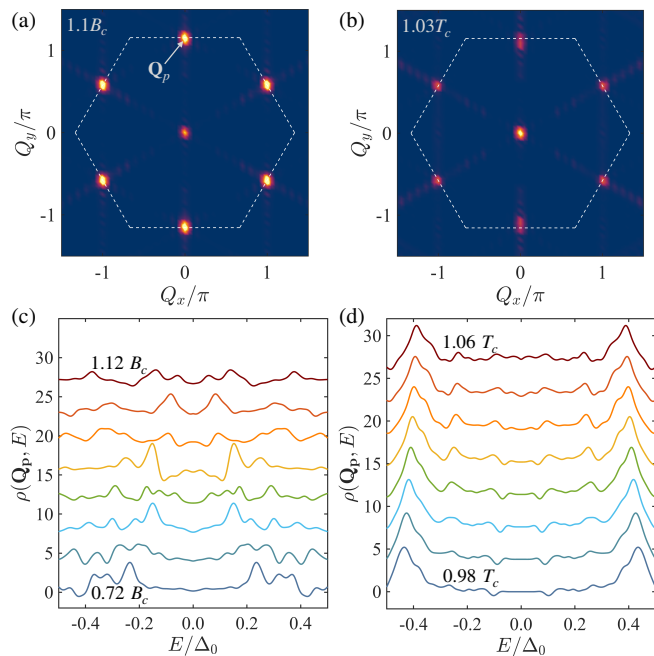


FIG. 5. Fourier transformed pair-pair correlation function $C(\mathbf{Q})$ at (a) magnetic field $B_z = 1.1B_c$, temperature $T = 0$, and (b) $B_z = 0$, $T = 1.03T_c$, indicating the presence of the CPDW correlation above the superconducting transition. (c), (d) Fourier-transformed local density of states $\rho(\mathbf{Q}_p, E)$ at a characteristic CPDW momentum \mathbf{Q}_p , shown in (a), at different values of B and T across the superconducting transition, revealing particle-hole symmetric quasiparticle states with a non-zero weight at $E = 0$. The results were obtained on a $20a \times 20a$ lattice with periodic boundary conditions. All other parameters are the same as in Fig. 2. A constant offset has been added to the vertical axis for each curve in (c) and (d) for clarity.

(Fig. 3(c)) in the pseudogap state. At the critical field B_c for vanishing n_s , $|\Delta|$ exhibits a dip while $\rho(E=0)$ shows a zero weight (inset in (Fig. 3(c))), attesting the appearance of an unconventional state immediately above B_c . The enhancement of the critical magnetic field and the appearance of the pseudogap in the CPDW state suggest that there is a correlation among these phenomena. The temperature driven transition to the normal state also reveals a similar pseudogap (Fig. 3(d)), though the variation of $\rho(E=0)$ with T is rather monotonic. Moreover, the V-shaped density of states and the multiple coherence peaks around the gap show similarities with those observed in the tunneling spectra [12–14].

CPDW correlation above superconducting transition.—

To gain insights into the origin of the pseudogap, the profile of the absolute value of the pairing gap at different fields across the superconducting transition was looked at in Fig. 4(a),(b),(c). It is found that above and in the vicinity of the critical magnetic field, the pairing gap is locally suppressed in charge-ordered clusters, stabilizing an emergent granular superconducting state in which the pairing gap survives locally even though the long-range superconducting phase coherence vanishes. The magnetization profile also reveals periodic modulation, and the interplay of magnetization and superconducting gap prevails in the entire granular superconducting phase [23]. The fourier-transformed pair-pair correlation function $C(\mathbf{Q})$ and the fourier-transformed local density of states $\rho(\mathbf{Q}_p, E)$ at \mathbf{Q}_p , one of the three characteristic momenta for the CPDW, were also investigated (Fig. 5(a)-(d)) across the superconducting transition. Interestingly, the CPDW correlation survives above the critical magnetic field B_c and critical temperature T_c . The observable $\rho(\mathbf{Q}_p, E)$ is particle-hole symmetric *i.e.* it is symmetric when $E \rightarrow -E$, above and in the vicinity of B_c and T_c , ruling out other possible mechanisms of the pseudogap such as charge order of electronic states or modulation due to electron scattering from a periodic potential. From these findings, it can be argued that the

modulations of the density of states in the pseudogap, observed in the experiments, are a consequence of the CPDW of s -wave Cooper pairs without a global phase coherence.

Discussion and conclusion.—The superconducting state can be influenced by multiple properties of the compounds such as the TRS breaking loop current, the rotational symmetry-breaking nematic order, fermi surface nesting, Coulomb interactions and sublattice interference [31–35]. Despite the complex nature of the pairing mechanism, there are growing experimental evidences in support of spin-singlet s -wave pairing such as the absence of a nodal state while transitioning from an anisotropic full-gap state to an isotropic full-gap state driven by impurity concentration [11], and the appearance of a prominent Hebel-Slichter coherence peak immediately below T_c [36]. The proposed CPDW of s -wave Cooper pairs, therefore, provides a natural explanation for many paradoxical experimental observations, including the pseudogap in the tunneling spectra.

To summarize, it is shown that a CPDW state of $2a \times 2a$ periodicity emerges spontaneously in the kagomé lattice due to the interplay of onsite spin-singlet superconductivity with a charge order of the same periodicity and an orbital loop current. The CPDW correlation survives beyond the superconducting transition in granular regions without global superconducting phase coherence, producing a V-shaped particle-hole symmetric density of states and pseudogap, which are otherwise indicative of a nodal unconventional pairing symmetry.

Acknowledgements.—The work was supported by Science and Engineering Research Board, India (Research Grant No. SRG/2023/001188). Numerical calculations were performed at the computing resources of PARAM Ganga at the Indian Institute of Technology Roorkee, provided by National Supercomputing Mission, implemented by C-DAC, and supported by the Ministry of Electronics and Information Technology and Department of Science and Technology, Government of India.

-
- [1] B. R. Ortiz, L. C. Gomes, J. R. Morey, M. Winiarski, M. Bordelon, J. S. Mangum, I. W. H. Oswald, J. A. Rodriguez-Rivera, J. R. Neilson, S. D. Wilson, E. Ertekin, T. M. McQueen, and E. S. Toberer, “New kagomé prototype materials: discovery of KV_3Sb_5 , RbV_3Sb_5 , and CsV_3Sb_5 ,” *Phys. Rev. Mater.* **3**, 094407 (2019).
- [2] B. R. Ortiz, S. M. L. Teicher, Y. Hu, J. L. Zuo, P. M. Sarte, E. C. Schueller, A. M. M. Abeykoon, M. J. Krogstad, S. Rosenkranz, R. Osborn, R. Seshadri, L. Balents, J. He, and S. D. Wilson, “ CsV_3Sb_5 : A Z_2 topological kagomé metal with a superconducting ground state,” *Phys. Rev. Lett.* **125**, 247002 (2020).
- [3] M. Shi, F. Yu, Y. Yang, F. Meng, B. Lei, Y. Luo, Z. Sun, J. He, R. Wang, Z. Jiang, Z. Liu, D. Shen, T. Wu, Z. Wang, Z. Xiang, J. Ying, and X. Chen, “A new class of bilayer kagomé lattice compounds with Dirac nodal lines and pressure-induced superconductivity,” *Nat. Commun.* **13**, 2773 (2022).
- [4] Y.-X. Jiang, J.-X. Yin, M. M. Denner, N. Shumiya, B. R. Ortiz, G. Xu, Z. Guguchia, J. He, M. S. Hossain, X. Liu, J. Ruff, L. Kautzsch, S. S. Zhang, G. Chang, I. Belopolski, Q. Zhang, T. A. Cochran, D. Multer, M. Litskevich, Z.-J. Cheng, X. P. Yang, Z. Wang, R. Thomale, T. Neupert, S. D. Wilson, and M. Z. Hasan, “Unconventional chiral charge order in kagomé superconductor KV_3Sb_5 ,” *Nat. Mater.* **20**, 1353 (2021).
- [5] C. Mielke, D. Das, J.-X. Yin, H. Liu, R. Gupta, Y.-X. Jiang, M. Medarde, X. Wu, H. C. Lei, J. Chang, P. Dai, Q. Si, H. Miao, R. Thomale, T. Neupert, Y. Shi, R. Khasanov, M. Z. Hasan, H. Luetkens, and Z. Guguchia, “Time-reversal symmetry-breaking charge order in a kagomé superconductor,” *Nature* **602**, 245 (2022).
- [6] R. Khasanov, D. Das, R. Gupta, C. Mielke, M. Elender, Q. Yin, Z. Tu, C. Gong, H. Lei, E. T. Ritz, R. M. Fernandes, T. Birol, Z. Guguchia, and H. Luetkens, “Time-reversal symmetry broken by charge order in CsV_3Sb_5 ,” *Phys. Rev. Res.* **4**, 023244 (2022).
- [7] H. Li, T. T. Zhang, T. Yilmaz, Y. Y. Pai, C. E. Marvinney, A. Said, Q. W. Yin, C. S. Gong, Z. J. Tu, E. Vescovo, C. S. Nelson, R. G. Moore, S. Murakami, H. C. Lei, H. N. Lee, B. J. Lawrie, and H. Miao, “Observation of unconventional charge density wave without acoustic phonon anomaly in kagomé superconductors AV_3Sb_5 ($A=Rb, Cs$),” *Phys. Rev. X* **11**, 031050 (2021).
- [8] M. M. Denner, R. Thomale, and T. Neupert, “Analysis of charge order in the kagomé metal AV_3Sb_5 ($A=K, Rb, Cs$),” *Phys. Rev. Lett.* **127**, 217601 (2021).
- [9] M. H. Christensen, T. Birol, B. M. Andersen, and R. M. Fernandes, “Theory of the charge density wave in AV_3Sb_5 kagomé metals,” *Phys. Rev. B* **104**, 214513 (2021).
- [10] Z. Guguchia, C. Mielke, D. Das, R. Gupta, J.-X. Yin, H. Liu, Q. Yin, M. H. Christensen, Z. Tu, C. Gong, N. Shumiya, M. S. Hossain, T. Gamsakhurdashvili, M. Elender, P. Dai, A. Amato, Y. Shi, H. C. Lei, R. M. Fernandes, M. Z. Hasan, H. Luetkens, and R. Khasanov, “Tunable unconventional kagomé superconductivity in charge ordered RbV_3Sb_5 and KV_3Sb_5 ,” *Nat. Commun.* **14**, 153 (2023).
- [11] M. Roppongi, K. Ishihara, Y. Tanaka, K. Ogawa, K. Okada, S. Liu, K. Mukasa, Y. Mizukami, Y. Uwatoko, R. Grasset, M. Konczykowski, B. R. Ortiz, S. D. Wilson, K. Hashimoto, and T. Shibauchi, “Bulk evidence of anisotropic s -wave pairing with no sign change in the kagomé superconductor CsV_3Sb_5 ,” *Nat. Commun.* **14**, 667 (2023).
- [12] H. Zhao, H. Li, B. R. Ortiz, S. M. L. Teicher, T. Park, M. Ye, Z. Wang, L. Balents, S. D. Wilson, and I. Zeljkovic, “Cascade of correlated electron states in the kagomé superconductor CsV_3Sb_5 ,” *Nature* **599**, 216 (2021).
- [13] H. Chen, H. Yang, B. Hu, Z. Zhao, J. Yuan, Y. Xing, G. Qian, Z. Huang, G. Li, Y. Ye, S. Ma, S. Ni, H. Zhang, Q. Yin, C. Gong, Z. Tu, H. Lei, H. Tan, S. Zhou, C. Shen, X. Dong, B. Yan, Z. Wang, and H.-J. Gao, “Roton pair density wave in a strong-coupling kagomé superconductor,” *Nature* **599**, 222 (2021).
- [14] H.-S. Xu, Y.-J. Yan, R. Yin, W. Xia, S. Fang, Z. Chen, Y. Li, W. Yang, Y. Guo, and D.-L. Feng, “Multiband superconductivity with sign-preserving order parameter in

- kagomé superconductor CsV_3Sb_5 ,” *Phys. Rev. Lett.* **127**, 187004 (2021).
- [15] H.-M. Jiang, M.-X. Liu, and S.-L. Yu, “Impact of the orbital current order on the superconducting properties of the kagome superconductors,” *Phys. Rev. B* **107**, 064506 (2023).
- [16] T. Kato, Y. Li, T. Kawakami, M. Liu, K. Nakayama, Z. Wang, A. Moriya, K. Tanaka, T. Takahashi, Yu. Yao, and T. Sato, “Three-dimensional energy gap and origin of charge-density wave in kagomé superconductor KV_3Sb_5 ,” *Commun. Mater.* **3**, 30 (2022).
- [17] R. Gupta, D. Das, C. Mielke, E. T. Ritz, F. Hotz, Q. Yin, Z. Tu, C. Gong, H. Lei, T. Birol, R. M. Fernandes, Z. Guguchia, H. Luetkens, and R. Khasanov, “Two types of charge order with distinct interplay with superconductivity in the kagomé material CsV_3Sb_5 ,” *Commun. Phys.* **5**, 232 (2022).
- [18] H. Tan, Y. Liu, Z. Wang, and B. Yan, “Charge density waves and electronic properties of superconducting kagomé metals,” *Phys. Rev. Lett.* **127**, 046401 (2021).
- [19] X. Feng, K. Jiang, Z. Wang, and J. Hu, “Chiral flux phase in the kagomé superconductor AV_3Sb_5 ,” *Sci. Bull.* **66**, 1384 (2021).
- [20] S.-Y. Yang, Y. Wang, B. R. Ortiz, D. Liu, J. Gayles, E. Derunova, R. Gonzalez-Hernandez, L. Šmejkal, Y. Chen, S. S. P. Parkin, S. D. Wilson, E. S. Toberer, T. McQueen, and M. N. Ali, “Giant, unconventional anomalous Hall effect in the metallic frustrated magnet candidate, KV_3Sb_5 ,” *Sci. Adv.* **6**, eabb6003 (2020).
- [21] Y. Gan, W. Xia, L. Zhang, K. Yang, X. Mi, A. Wang, Y. Chai, Y. Guo, X. Zhou, and M. He, “Magneto-Seebeck effect and ambipolar Nernst effect in the CsV_3Sb_5 superconductor,” *Phys. Rev. B* **104**, L180508 (2021).
- [22] F. H. Yu, T. Wu, Z. Y. Wang, B. Lei, W. Z. Zhuo, J. J. Ying, and X. H. Chen, “Concurrence of anomalous Hall effect and charge density wave in a superconducting topological kagomé metal,” *Phys. Rev. B* **104**, L041103 (2021).
- [23] See Supplemental Materials for more information.
- [1] D. J. Scalapino, S. R. White, and S. C. Zhang, “Superfluid density and the Drude weight of the Hubbard model,” *Phys. Rev. Lett.* **68**, 2830 (1992).
- [25] F. H. Yu, D. H. Ma, W. Z. Zhuo, S. Q. Liu, X. K. Wen, B. Lei, J. J. Ying, and X. H. Chen, “Unusual competition of superconductivity and charge-density-wave state in a compressed topological kagomé metal,” *Nat. Commun.* **12**, 3645 (2021).
- [26] B. S. Chandrasekhar, “A note on the maximum critical field of high-field superconductors,” *Appl. Phys. Lett.* **1**, 7 (1962).
- [27] A. M. Clogston, “Upper limit for the critical field in hard superconductors,” *Phys. Rev. Lett.* **9**, 266 (1962).
- [28] P. Fulde and R. A. Ferrell, “Superconductivity in a strong spin-exchange field,” *Phys. Rev.* **135**, A550 (1964).
- [29] A. I. Larkin and Y. N. Ovchinnikov, “Nonuniform state of superconductors,” *Zh. Eksp. Teor. Fiz* **47**, 1136 (1964).
- [30] R. C. Bruno and B. B. Schwartz, “Magnetic field splitting of the density of states of thin superconductors,” *Phys. Rev. B* **8**, 3161 (1973).
- [31] Y. Xiang, Q. Li, Y. Li, W. Xie, H. Yang, Z. Wang, Y. Yao, and H.-H. Wen, “Twofold symmetry of c -axis resistivity in topological kagomé superconductor CsV_3Sb_5 with in-plane rotating magnetic field,” *Nat. Commun.* **12**, 6727 (2021).
- [32] J.-T. Jin, K. Jiang, H. Yao, and Y. Zhou, “Interplay between pair density wave and a nested Fermi surface,” *Phys. Rev. Lett.* **129**, 167001 (2022).
- [33] L. Nie, K. Sun, W. Ma, D. Song, L. Zheng, Z. Liang, P. Wu, F. Yu, J. Li, M. Shan, D. Zhao, S. Li, B. Kang, Z. Wu, Y. Zhou, K. Liu, Z. Xiang, J. Ying, Z. Wang, T. Wu, and X. Chen, “Charge-density-wave-driven electronic nematicity in a kagomé superconductor,” *Nature* **604**, 59 (2022).
- [34] S. Zhou and Z. Wang, “Chern Fermi pocket, topological pair density wave, and charge-4e and charge-6e superconductivity in kagomé superconductors,” *Nat. Commun.* **13**, 7288 (2022).
- [35] X. Wu, T. Schwemmer, T. Müller, A. Coniglio, G. Sangiovanni, D. Di Sante, Y. Iqbal, W. Hanke, A. P. Schnyder, M. M. Denner, M. H. Fischer, T. Neupert, and R. Thomale, “Nature of unconventional pairing in the kagomé superconductors AV_3Sb_5 ($A=\text{K}, \text{Rb}, \text{Cs}$),” *Phys. Rev. Lett.* **127**, 177001 (2021).
- [36] C. Mu, Q. Yin, Z. Tu, C. Gong, H. Lei, Z. Li, and J. Luo, “S-wave superconductivity in kagomé metal CsV_3Sb_5 revealed by 121/123 Sb NQR and 51V NMR measurements,” *Chinese Phys. Lett.* **38**, 077402 (2021).

Supplemental Materials for "Chiral pair density wave as a precursor of the pseudogap in kagomé superconductors"

1. Robustness of the CPDW state

The CPDW state, discussed in the main text, appears also for smaller values of the attractive pair-wise interaction strength \mathcal{U} , as shown in Fig. S1(a), (b), (c). The discrepancy between the pairing amplitude and the superfluid density exists at smaller values of \mathcal{U} , as shown in Fig. S1(d). Similarly, different sets of the charge-order strength μ_{co} and loop current parameter t_{lc} also give rise to the CPDW state and the pseudogap behavior near the superconducting transition. Fig. S2 shows the Fourier transformed pair-pair correlation function $C(\mathbf{Q})$ for two sets of μ_{co} and t_{lc} , showing the C3-symmetric CPDW correlations.

2. Self-consistent gap equation

The superconducting order parameter, the local pairing gap $\Delta(\mathbf{r}_i) = -\mathcal{U}\langle c_{i\uparrow}c_{i\downarrow} \rangle$, can be re-written using the Bogoliubov-Valatin transformation $c_{i\sigma} = \sum_n u_{ni}^\sigma \gamma_n + v_{ni}^{\sigma*} \gamma_n^\dagger$, where γ_n is fermionic annihilation operator acting on the n^{th} eigenstate and u_{ni}^σ (v_{ni}^σ) is the corresponding quasiparticle (quasihole) amplitude at site i and spin σ , as

$$\Delta(\mathbf{r}_i) = -\mathcal{U} \sum_n [u_{ni}^\uparrow v_{ni}^{\downarrow*} (1 - f(E_n)) + u_{ni}^\downarrow v_{ni}^{\uparrow*} f(E_n)] \quad (\text{E1})$$

where $f(E_n)$ is the fermi function corresponding to the n^{th} eigen-energy E_n . Using the relation $f(x) = \frac{1}{2} - \frac{1}{2} \tanh\left(\frac{x}{2}\right)$, the above equation can be expressed as

$$\Delta(\mathbf{r}_i) = \frac{\mathcal{U}}{2} \sum_n [u_{ni}^\uparrow v_{ni}^{\downarrow*} - u_{ni}^\downarrow v_{ni}^{\uparrow*}] \tanh\left(\frac{E_n}{2k_B T}\right), \quad (\text{E2})$$

where k_B is the Boltzmann constant and T is the temperature. In the above equation, the energy-independent terms were dropped because the contribution from those terms will vanish. The above equation is the self-consistent gap equation used in the calculations. The self-consistency iteration is performed until convergence is achieved at each lattice sites.

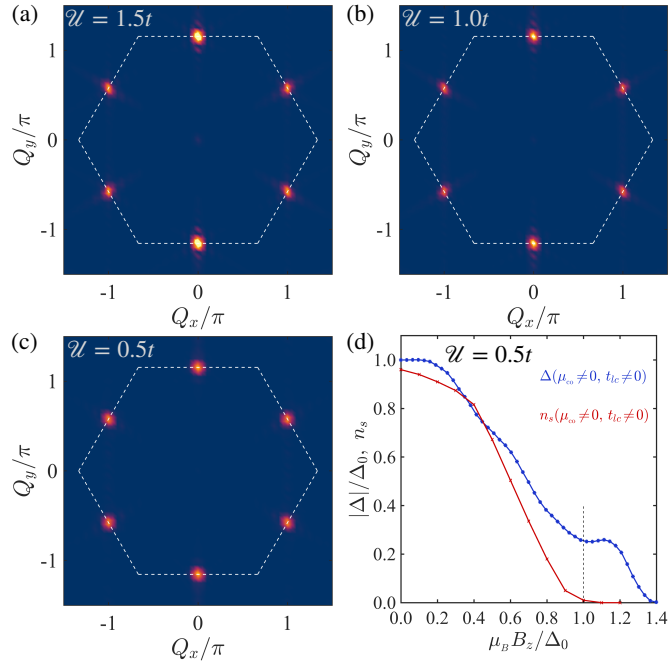


FIG. S1. (a)-(c) Fourier transformed pair-pair correlation function $C(\mathbf{Q})$ at different values of \mathcal{U} : (a) $\mathcal{U} = 1.5t$, (b) $\mathcal{U} = 1.0t$, and (c) $\mathcal{U} = 0.5t$. (d) Normalized pairing gap magnitude $|\Delta|/\Delta_0$ and the superfluid density n_s as a function of the magnetic field B_z . The results were obtained on a $20a \times 20a$ lattice with periodic boundary conditions. All other parameters are the same as in Fig. 1 of the main text.

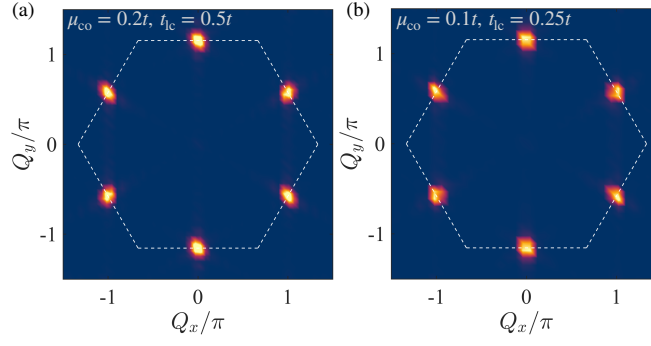


FIG. S2. Fourier transformed pair-pair correlation function $C(\mathbf{Q})$ at different values of the charge-order strength μ_{co} and loop current parameter t_{lc} : (a) $\mu_{co}=0.2t$, $t_{lc}=0.5t$, and (b) $\mu_{co}=0.1t$, $t_{lc}=0.25t$. The results were obtained on a $20a \times 20a$ lattice with periodic boundary conditions. All other parameters are the same as in Fig. 1 of the main manuscript.

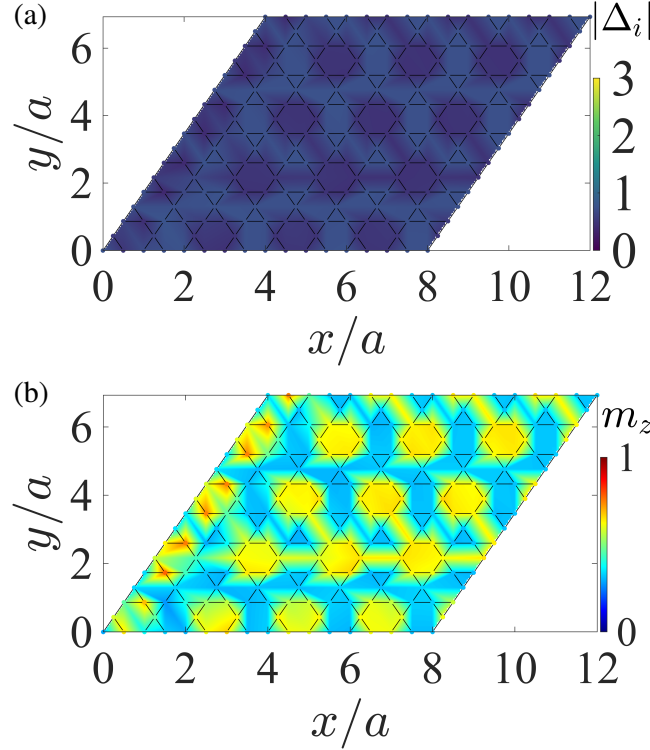


FIG. S3. Profile of the absolute value of the pairing gap (top panel) and z component of magnetization (bottom panel) at $B=1.1B_c$. All other parameters are the same as in Fig.4 of the main text.

3. Calculation of superfluid density

The superfluid density is given by the effective Drude weight, derived earlier in Ref. [R1]

$$n_s = \frac{D_s}{\pi e^2} = -\langle \kappa \rangle + \Lambda(\mathbf{Q} \rightarrow 0, i\omega \rightarrow 0), \quad (\text{E3})$$

where the first term on the right hand side is the diamagnetic response and the second term is the paramagnetic response. The diamagnetic term, associated with the local kinetic energy, can be expressed in terms of the Bogoliubov-de Gennes (BdG) quasiparticle weights as

$$\begin{aligned} \kappa_i = -t \sum_{\langle j \rangle, n, \sigma} & [u_{ni}^\sigma u_{nj}^{\sigma*} + c.c.] f(E_n) \\ & + [v_{ni}^\sigma v_{nj}^{\sigma*} + c.c.] (1 - f(E_n)). \end{aligned} \quad (\text{E4})$$

The paramagnetic response is given by the transverse current-current correlation function

$$\Lambda(\mathbf{Q}, \omega_n) = \frac{1}{N} \int_0^{1/T} e^{i\omega_n \tau} \langle j_x^p(\mathbf{Q}, \tau) j_x^p(-\mathbf{Q}, 0) \rangle d\tau, \quad (\text{E5})$$

with $\omega_n = 2\pi nT$ and the paramagnetic current $j_x^p(\mathbf{Q})$ is given by

$$j_x^p(\mathbf{Q}) = it \sum_{i,\sigma} (c_{i+\hat{x},\sigma}^\dagger c_{i,\sigma} - c_{i,\sigma}^\dagger c_{i+\hat{x},\sigma}) e^{-\mathbf{Q} \cdot \mathbf{r}_i}. \quad (\text{E6})$$

The uniform (i.e. $\mathbf{Q}=0$) paramagnetic response can be obtained [R1], in terms of the BdG quasiparticle weights as

$$\begin{aligned} \Lambda(\mathbf{Q} \rightarrow 0, i\omega \rightarrow 0) &= \frac{1}{N} \sum_{i,j,n_1,n_2}^{\sigma,\sigma'} \mathcal{A}_{n_1 n_2}^{i\sigma\sigma'} [\mathcal{A}_{n_1 n_2}^{j\sigma\sigma'*} + \mathcal{B}_{n_1 n_2}^{j\sigma\sigma'}] \\ &\quad \times \frac{f(E_{n_1}) - f(E_{n_2})}{E_{n_1} - E_{n_2}}, \end{aligned} \quad (\text{E7})$$

where N is the total number of lattice sites and

$$\begin{aligned} \mathcal{A}_{n_1 n_2}^{i\sigma\sigma'} &= 2[u_{n_1 j}^{\sigma'*} u_{n_2 i}^\sigma - u_{n_1 i}^{\sigma*} u_{n_2 j}^{\sigma'}], \\ \mathcal{B}_{n_1 n_2}^{i\sigma\sigma'} &= 2[v_{n_1 j}^{\sigma'*} v_{n_2 i}^\sigma - v_{n_1 i}^{\sigma*} v_{n_2 j}^{\sigma'}]. \end{aligned} \quad (\text{E8})$$

4. Magnetization in the emergent granular state

Near the critical magnetic field B_c for the superconducting transition (as dictated by the vanishing superfluid density), the system goes through an emergent granular phase in which the superconducting gap magnitude is suppressed in the charge-ordered clusters, as shown in Fig. S3(a) (and Fig.4 in the main text). The magnetization profile, obtained via $m_{zi} = c_{i\uparrow}^\dagger c_{i\uparrow} - c_{i\downarrow}^\dagger c_{i\downarrow}$, shown in Fig. S3(b), also reveals a periodic modulation. The magnetization is enhanced slightly in the regions in which the pairing amplitude is decreased. This interplay of magnetization and superconducting order parameter exists in the entire granular superconducting phase, without any long-range superconducting phase coherence.

5. Effect of loop current in the density of states

To explore the role of the loop current in formation of the pseudogap near the superconducting transition and to understand the finite size effect, in Fig. S4 the density of states has been presented for loop current magnitude t_{lc} and different lattice sizes. The results show that, despite the little noise in the density of state originating due to finite size effect, it is evident that quasiparticle states build up within the superconducting gap due to the loop current.

[R1] D. J. Scalapino, S. R. White, and S. C. Zhang, "Superfluid density and the Drude weight of the Hubbard model," Phys. Rev. Lett. **68**, 2830 (1992).

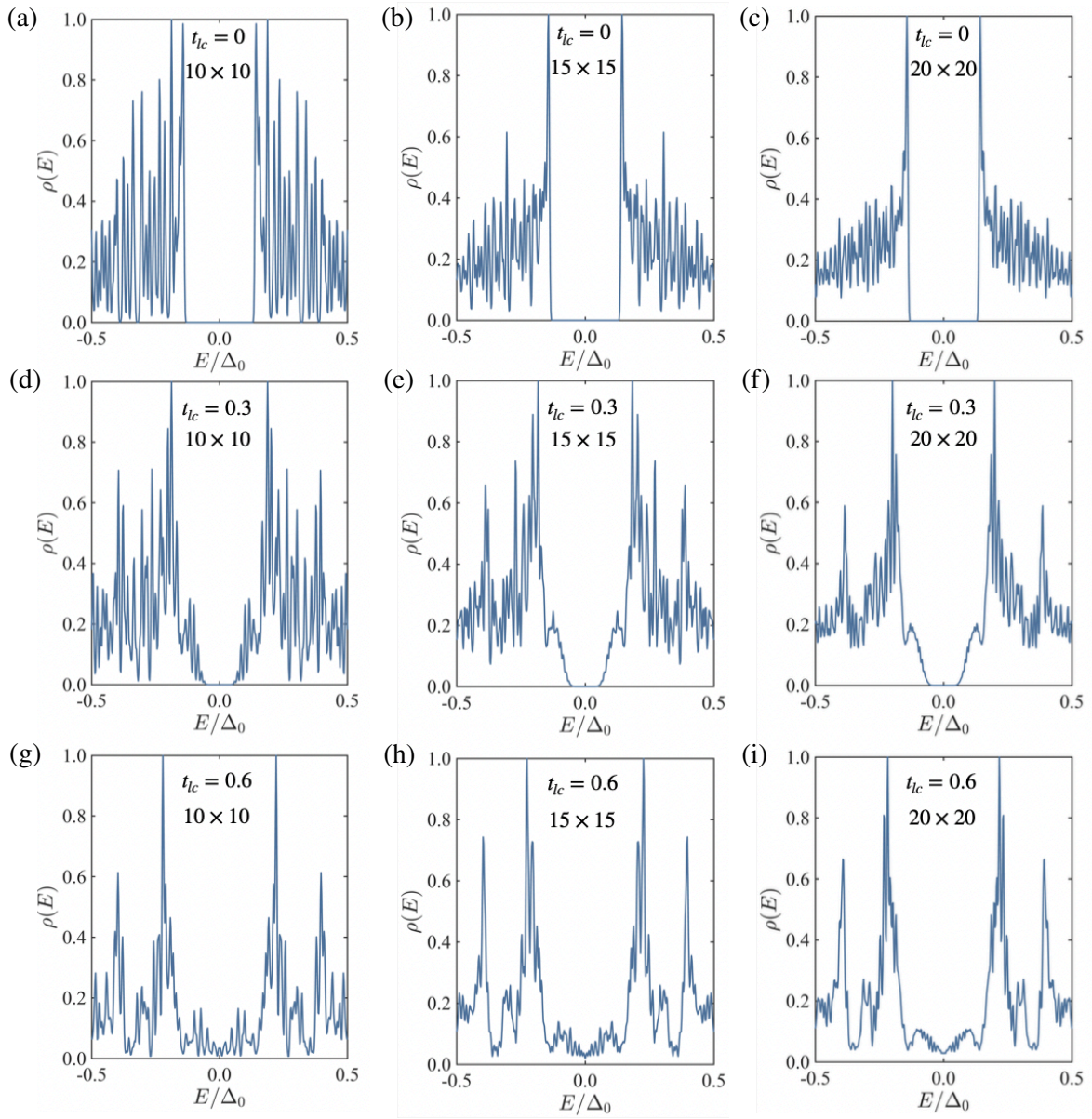


FIG. S4. Density of states of a kagome lattice with periodic boundary conditions for different lattice sizes (different columns) and different values of the loop current amplitude t_{lc} (different rows), without chemical potential modulation and at a magnetic field $B=2t$.